Hiriyalu Shivegowda Ashrith,[1] Mrityunjay Doddamani,[1] Vinayak Neelakanth Gaitonde,[2] and Nikhil Gupta[3]

Influence of Materials and Machining Parameters on Drilling Performance of Syntactic Foams

[1] Lightweight Materials Laboratory, Department of Mechanical Engineering, National Institute of Technology Karnataka, PO Srinivasnagar, Surathkal 575025, India

[2] Department of Industrial and Production Engineering, B.V.B. College of Engineering and Technology, KLE Technological University, Hubballi, Karnataka 580031, India

[3] Composite Materials and Mechanics Laboratory, Mechanical and Aerospace Engineering Department, Tandon School of Engineering, New York University, 6 MetroTech Center, Brooklyn, NY 11201, USA (Corresponding author), e-mail: ngupta@nyu.edu, https://orcid.org/0000-0001-7128-4459

ABSTRACT

The effects of drilling parameters and material properties are investigated on epoxy matrix syntactic foams reinforced with 20, 40, and 60 volume percent glass microballoon. The influences of cutting speed, feed, drill diameter, and filler content on drilling performance are studied based on the full factorial design of experiments using tungsten carbide twist drills. Based on experimental results, machinability aspects within the range of the chosen input parameters are predicted using response surface methodology-based models, which can guide industrial practitioners for choosing the appropriate process parameters. Microscopy is conducted on the drilled specimens to understand crack initiation and propagation mechanisms. The thrust force and specific cutting coefficient of syntactic foam are 40 % lower as compared to those of neat epoxy. The surface roughness of syntactic foams is higher than that of neat epoxy. The micrographs of drill bits show negligible tool wear. These results show the possibility of using syntactic foams in industrial applications in which the drilling of material is required for reasons such as joining using bolts.

Nomenclature

η = radius ratio

ρ_{MB} = glass microballoon (GMB) density (kg/m^3)

ρ_g = glass density (kg/m^3)

w = GMB wall thickness (µm)

ρ_t = theoretical density of syntactic foams (kg/m^3)

ρ_e = experimental density of syntactic foams (kg/m^3)

$\Phi_{\mu P}$ = GMB porosity (volume %)

K_f = specific cutting coefficient (MPa)

Φ_v = matrix porosity (volume %)

Φ_t = total porosity (volume %)

v = cutting speed (m/min)

f = feed (mm/rev)

R = filler content (volume %)

D = drill diameter (mm)

F_t = thrust force (N)

R_a = surface roughness (µm)

N = spindle speed (r/min)

Introduction

Lightweight composite materials called syntactic foams are synthesized by dispersing hollow microballoons in a matrix resin [1–3]. Syntactic foams have helped in increasing fuel efficiency and pay load capacity as well as reducing emissions [4–9] in transportation applications [10–13]. Syntactic foams are also used as structural components and buoyancy modules in underwater vehicle structures [14], where holes are drilled for screws and bolts to assemble different sections and install various components. The presence of abrasive fillers like glass microballoons (GMBs) [15] may lead to higher tool wear and poor surface finish, which need to be characterized for such applications. The quality of the drilled hole strongly depends on the process parameters and drilling conditions. Poor hole quality leads to a 60 % rejection of fibrous composite parts in the manufacturing industry, substantially increasing the overall production cost [16]. The optimization of drilling procedures will be useful in helping the adoption of syntactic foams in new structural applications.

A comprehensive review of the effects of feed, speed, drill wear, drill geometry, and workpiece composition on machinability characteristics such as thrust force, torque, and surface roughness in the drilling of fiber-reinforced polymer matrix composites is available in published literature [17]. It is observed that increasing the cutting speed leads to increased thrust force in the drilling of carbon fiber-reinforced polymer (CFRP) composites and that the twist drills provide better machinability characteristics than multifacet drills [18]. The effects of cutting speed, feed, and drill size on thrust force, torque, and surface roughness on the drilling of glass fiber-reinforced polymer (GFRP) composites have been studied [19,20]. Results reveal that the cutting speed and drill diameter have a significant effect on the thrust force, while torque is highly influenced by the drill diameter and specimen thickness. In addition, the feed and drill size have a significant effect on the surface

roughness of the drilled holes, whereas the feed and cutting speed are found to significantly influence the delamination in the drilling of GFRP composites [21,22].

Available studies that focus on the effects of cutting speed and feed in the drilling of reinforced and unreinforced polyamide have used full factorial design (FFD)- and response surface methodology (RSM)-based models to analyze the surface roughness of drilled holes [23]. The surface roughness of the reinforced polyamide is found to be lower than that of the matrix at all levels of process parameters. Reinforced polyamide provides a better surface finish at a low feed and intermediate cutting speed. Analysis of variance (ANOVA) and genetic algorithms have been used to analyze and optimize the effect of process parameters on hole quality in the drilling of CFRP [24]. Results reveal that the feed rate significantly influences the thrust force, push-out delamination, and diameter of the hole, but the circularity of the drilled hole is greatly influenced by the spindle speed.

A study on the effect of spindle speed, drill geometry, and feed on thrust force, hole diameter, and circularity error found that the optimum conditions were different in the drilling of unreinforced and reinforced polyamides [25]. An investigation on the effect of spindle speed and feed on machinability characteristics like cutting force, surface roughness, tool wear, and burr formation found that the unreinforced polyamides show better machinability characteristics than reinforced polyamides [26]. The influence of speed, feed, and tool coating on thrust force and tool wear is analyzed in the drilling of GFRP composites [27]. A cemented carbide tool exhibits superior wear resistance in comparison to a high-speed steel tool. An analytical model to predict the critical thrust force responsible for delamination in drilling CFRP laminates has been proposed [28,29], which can be useful in predicting trends.

Despite the availability of exhaustive literature on the drilling of fiber-reinforced composites, studies on the drilling of syntactic foams are not yet available, which is the focus of this work. Based on the experimental results, RSM-based models for thrust force, surface roughness, and specific cutting coefficient are developed to analyze the influence of cutting speed, feed, drill diameter, and GMB content. ANOVA is used to validate the developed models.

Materials and Methods

CONSTITUENT MATERIALS

LAPOX L-12 epoxy resin with K-6 hardener, supplied by Atul Ltd., Valsad, Gujarat, India, is used as the matrix. GMBs of grade SID-350 (Trelleborg Offshore, Boston, MA), with a nominal true particle density of 350 kg/m^3 and an average diameter of 45 µm, are used as filler. The radius ratio for the GMBs is calculated using the following [30]:

$$\eta = \left(1 - \frac{\rho_{MB}}{\rho_g}\right)^{1/3}$$

(1)

where glass density is taken as 2,540 kg/m^3 [31]. The radius ratio is used to calculate the nominal wall thickness and radius ratio of GMBs as 1.080 µm and 0.952, respectively [32].

SAMPLE PREPARATION

Syntactic foams with 20, 40, and 60 volume percent (vol.%) of GMBs are fabricated by mixing a weighed quantity of GMBs in the epoxy monomer and stirring slowly until a homogeneous slurry is formed. The hardener (10 weight percent) is added into the slurry, and the mixture is stirred for 5 minutes and then degassed prior to pouring into molds

with a 35-mm diameter and 16-mm height. A silicone release agent is applied to the mold surfaces. The specimens are cured for 24 h at room temperature and then post-cured for 2 h at 90°C. Neat epoxy specimens are also prepared under similar processing conditions for comparison. In total, 81 specimens are prepared for each volume fraction. The specimens are coded according to the convention EZZ, where E and ZZ denote the epoxy matrix and vol.% of the filler, respectively.

DENSITY AND POROSITY MEASUREMENTS

The specimen density is measured according to ASTM C271-16, *Standard Test Method for Density of Sandwich Core Materials*. The density of the neat epoxy is measured to be 1,192 kg/m^3, which is used in the rule of mixtures to estimate the theoretical density (ρ_t) of syntactic foams [33]. Ignoring the fraction of crushed GMBs during syntactic foam synthesis, the entrapped matrix porosity (Φ_v) is estimated by the following:

$$\Phi_v = \frac{\rho_t - \rho_e}{\rho_t} \times 100 \tag{2}$$

The volume fraction of GMB porosity in syntactic foams is calculated by the following:

$$\Phi_{\mu P} = R \times \eta^3 \tag{3}$$

The total porosity of syntactic foams (Φ_t) is a summation of the matrix and GMB porosities. Higher theoretical densities of syntactic foams than experimental values, as seen from **Table 1**, indicate air entrapment in the matrix and insignificant GMB crushing during fabrication. Ignoring the content of the particles crushed during processing, calculations show the matrix porosity to be less than 9 vol.% with an increasing trend in GMB content (see **Table 1**). Density reduction in the range of 18–48 % is noted for syntactic foams with respect to the neat resin density. Representative micrographs of syntactic foams with the lowest and highest GMB contents are presented in **Fig. 1**. GMBs are observed to be uniformly dispersed in the matrix. No particle debris embedded in the epoxy resin is observed, affirming the fact that the damage and fracture of GMBs during processing was not significant.

PLANNING OF EXPERIMENTS

A total of 81 experiments are planned based on the FFD with three replicates for each condition [34]. The values of experimental parameters used for proposing a regression model are based on RSM, which has been used previously in the modeling of drilling behavior [23,35,36]. Using RSM with a statistical design of experiment approach, the individual and interaction effects of input parameters can be obtained with the minimum number of experiments [37]. The model can be written as follows [34]:
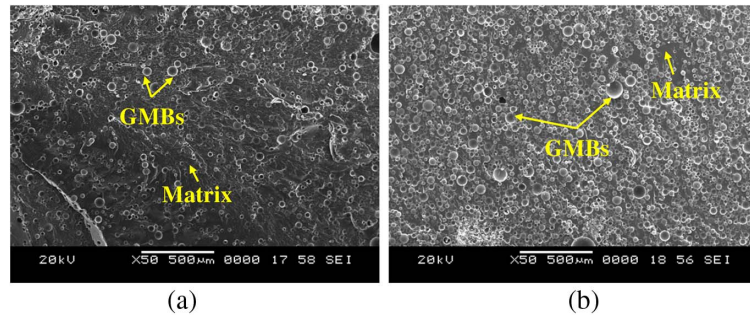
TABLE 1

Density and porosity estimations of neat epoxy and syntactic foams.

Sample Type	ρ_t	ρ_e	Φ_v	$\Phi_{\mu P}$	Φ_t	Density Difference Compared to Epoxy, %
E	1,192	1,192	0.0	0.0	0.0	–
E20	1,023.6	977.33 ± 2.56	4.52	17.26	21.78	18.01
E40	855.2	798.07 ± 8.65	6.68	34.51	41.19	33.05
E60	686.8	625.26 ± 12.45	8.96	51.77	60.73	47.55

(a)   (b)

$$Y = \varphi(x_1, x_2, x_3, \ldots \ldots, x_k) \qquad (4)$$

where Y is the response, $x_1, x_2, x_3, \ldots, x_k$ are the input variables, and φ is the response function. In the present investigation, the cutting speed, feed, drill diameter, and filler content are considered as independent variables, while the thrust force (F_t), surface roughness (R_a), and specific cutting coefficient (K_f) are considered as dependent variables. The levels of the chosen input parameters are selected based on the earlier studies [10,19,22,34,38–40] and are presented in Table 2. The second order RSM-based model is generated using experimental data to find the effects of the intermediate process parameter on the responses and is expressed as follows [34]:

$$Y = b_0 + b_1 \times v + b_2 \times f + b_3 \times D + b_4 \times R + b_{11} \times v^2 + b_{22} \times f^2$$
$$+ b_{33} \times D^2 + b_{44} \times R^2 + b_{12} \times v \times f + b_{13} \times v \times D + b_{14} \times v$$
$$\times R + b_{23} \times f \times D + b_{24} \times f \times R + b_{34} \times D \times R \qquad (5)$$

where b_o, $b_1, \ldots b_{34}$ are the regression coefficients to be determined. The regression coefficients of the quadratic model are determined by the following [34]:

$$B = (X^T X)^{-1} X^T Y \qquad (6)$$

where B is a matrix of parameter estimates; X is calculation matrix that includes linear, quadratic, and interaction terms; X^T is the transpose of X; and Y is a matrix of response.

TABLE 2

Process parameters and their levels for neat epoxy and syntactic foams [10,19,22,38–40].

	Level		
Parameters	1	2	3
v^a	25	75	125
f^a	0.04	0.08	0.12
D^a	8	12	16
R^b	20	40	60

Note: [a] Neat epoxy; [a, b] Syntactic foams.

DRILLING EXPERIMENTS

Drilling experiments are conducted as per FFD of experiments with coated solid tungsten carbide twist drills of diameters 8, 12, and 16 mm fitted on a vertical CNC machine with the specifications listed in Table 3, along with the specifications of the dynamometer used to measure the thrust force. The surface roughness of the drilled hole is measured using a Mitutoyo surftest (SJ 301, Mitutoyo Corporation, Sakado, Kawasaki, Kanagawa, Japan) with a 0.8-mm cut-off length. The specific cutting coefficient (K_f) is defined as the ratio of total energy input rate to material removal rate and is given by the following:

$$K_f = \frac{2 \times F_t}{f \times D} \tag{7}$$

The input parameters (I) and their levels (L) are coded together as I_L. For example, D_{12} represents a drill diameter of 12 mm.

IMAGING

A microstructural examination is carried out using a scanning electron microscope (JSM 6380LA, JEOL Ltd., Akishima, Tokyo, Japan). A JFC-1600 auto fine coater (JEOL Ltd., Akishima, Tokyo, Japan) is used to sputter-coat the samples with gold. A confocal microscope (LEXT, OLS4000, Olympus Corporation, Shinjuku, Tokyo, Japan) is used for inspecting the drilling tool.

Results and Discussion

EXPERIMENTAL INVESTIGATION

Table 4 presents the experimentally measured values of the drilling responses for the neat epoxy and syntactic foams. The thrust force increases with increase in the cutting speed, feed, and drill diameter, while it decreases with increase in the filler loadings. The resistance offered by the workpiece increases with increases in the feed, resulting in higher thrust forces [41]. The contact area of the drilled hole increases with the drill diameter, increasing F_t [19]. Fig. 2a and b shows the schematic representation of the drilling

TABLE 3

Machine tool specification used in the drilling study.

	Machining Center		Drilling Tool Dynamometer
Make	MTAB Engineers Pvt. Ltd., Perungudi, Chennai, India	Make	Syscon Instruments Pvt. Ltd., Bangalore, Karnataka, India
Model	MAX MILL PLUS+	Product	Drill Tool Sensors
Voltage	415 V ± 2 %, 3 Phase	type	Strain gauge
Axis travel ($X \times Y \times Z$)	$480 \times 360 \times 500$ mm	Voltage	230 V AC, 50 Hz, 1 Phase
Table size ($L \times W$)	600×350 mm	Maximum thrust	500 kg
Max. table load	250 kg	Maximum torque	10 kg-m
Control system	Fanuc Oi Mate MD	Safe overload	125 % of rated capacity
Max. spindle speed	9,000 r/min	Maximum overload	150 % of rated capacity
Spindle motor power	7.5 kW	Fatigue rating	10 E6 full cycles
Axis accuracy	0.01 mm	Excitation maximum	10 VDC
Axis repeatability	± 0.005 mm	Sensitivity	1 mV/V (Nominal)
Rapid feed	30 m/min	Temperature range	10°C to 50°C
Programmable feed rate	0–6,000 mm/min		

mechanism in syntactic foams. As the drill bit advances, GMBs present next to the lip get de-bonded or sheared, resulting in crack and debris formation. These cracks in the brittle matrix lead to a lower thrust force [41], and such an effect enhances with increase in the filler content (see **Fig. 2b**). The micrograph in **Fig. 2c** shows the virgin and drilled hole surface of a representative E20 at an intermediate drilling step to check the crack initiation. Cracks are visible in the matrix at the GMB/epoxy interface in **Fig. 2d**. Plastic deformation in the form of chip formation with debris is evident in this micrograph.

The cutting speed has no measurable effect on the surface roughness of the hole in a neat epoxy specimen. However, the surface roughness of syntactic foams increases with cutting speed. Increasing cutting speed results in a rough surface due to a rise in the tool–workpiece interface temperature [23]. Surface roughness decreases with increase in the feed in both neat epoxy and syntactic foams. Reduced contact time between the tool and workpiece at a higher feed decreases interface temperature, reducing R_a [42]. **Fig. 2e** and **f** presents the surface texture of the drilled hole wall. Foams exhibit a higher surface roughness as compared to neat epoxy samples due to the presence of broken GMBs, as observed in **Fig. 2f**. GMB debris and the exposed matrix voids result in higher surface roughness values of syntactic foams as compared to the neat resin surface (see

TABLE 4

Experimental layout plan and measured F_t, R_a, and K_f values for neat epoxy and their syntactic foams.

Process Parameter			E			E20			E40			E60		
v, m/min	f, mm/rev	D, mm	F_t, N	R_a, μm	K_f, MPa	F_t, N	R_a, μm	K_f, MPa	F_t, N	R_a, μm	K_f, MPa	F_t, N	R_a, μm	K_f, MPa
	0.04	8	49.05	0.21	306.56	39.24	2.06	245.25	39.24	2.94	245.25	29.43	2.77	183.93
		12	98.10	0.15	408.75	68.67	1.44	286.12	68.67	1.12	286.12	49.05	0.86	204.37
		16	137.34	0.13	429.18	127.53	1.55	398.53	88.29	2.23	275.90	78.48	2.10	245.25
	0.08	8	88.29	0.14	275.90	58.86	2.30	183.93	49.05	2.33	153.28	39.24	2.22	122.62
25		12	127.53	0.12	265.68	88.29	1.26	183.93	68.67	1.21	143.06	58.86	0.78	122.62
		16	176.58	0.16	275.90	156.96	1.70	245.25	117.72	2.63	183.93	98.10	1.14	153.28
	0.12	8	98.10	0.15	204.37	68.67	3.32	143.06	58.86	2.38	122.62	39.24	1.92	81.75
		12	156.96	0.17	218.00	107.91	1.29	149.87	88.29	1.07	122.62	68.67	1.00	95.37
		16	215.82	0.16	224.81	166.77	1.32	173.71	127.53	1.55	132.84	98.10	1.11	102.18
	0.04	8	58.86	0.14	367.87	39.24	2.86	245.25	39.24	2.56	245.25	29.43	2.96	183.93
		12	98.10	0.14	408.75	78.48	1.49	327.00	58.86	1.65	245.25	39.24	1.77	163.50
		16	147.15	0.15	459.84	117.72	2.89	367.87	78.48	2.23	245.25	68.67	2.65	214.59
	0.08	8	88.29	0.14	275.90	58.86	3.24	183.93	49.05	2.10	153.28	39.24	3.00	122.62
75		12	137.34	0.18	286.12	107.91	1.65	224.81	78.48	1.26	163.50	68.67	1.54	143.06
		16	186.39	0.12	291.23	147.15	2.21	229.92	117.72	2.38	183.93	107.91	1.71	168.60
	0.12	8	107.91	0.13	224.81	68.67	3.42	143.06	58.86	3.30	122.62	49.05	2.39	102.18
		12	166.77	0.12	231.62	107.91	1.08	149.87	88.29	1.44	122.62	68.67	1.44	95.37
		16	225.63	0.20	235.03	176.58	2.41	183.93	137.34	2.42	143.06	117.72	2.56	122.62
	0.04	8	68.67	0.12	429.18	49.05	3.03	306.56	29.43	3.45	183.93	19.62	3.58	122.62
		12	107.91	0.22	449.62	88.29	1.22	367.87	58.86	2.01	245.25	49.05	1.33	204.37
		16	156.96	0.12	490.50	117.72	3.87	367.87	88.29	3.51	275.90	78.48	1.90	245.25
	0.08	8	98.10	0.12	306.56	68.67	3.34	214.59	49.05	3.61	153.28	39.24	4.75	122.62
125		12	156.96	0.16	327.00	88.29	1.29	183.93	78.48	1.32	163.50	68.67	1.66	143.06
		16	215.82	0.13	337.21	176.58	1.90	275.90	127.53	3.44	199.26	107.91	1.41	168.60
	0.12	8	107.91	0.13	224.81	98.10	3.51	204.37	58.86	3.47	122.62	49.05	3.68	102.18
		12	176.58	0.13	245.25	107.91	1.46	149.87	98.10	1.21	136.25	78.48	1.00	109.00
		16	245.25	0.12	255.46	186.39	3.21	194.15	156.96	2.80	163.50	117.70	1.26	122.62

FIG. 2

Schematic representation of drilling in (a) E20 and (b) E60 samples. (c,d) Scanning electron micrographs showing intermittent crack formation on drilled surface of E20 sample at different magnifications. Micrography of hole wall surface post drilling in (e) neat epoxy and (f) E60 specimens.
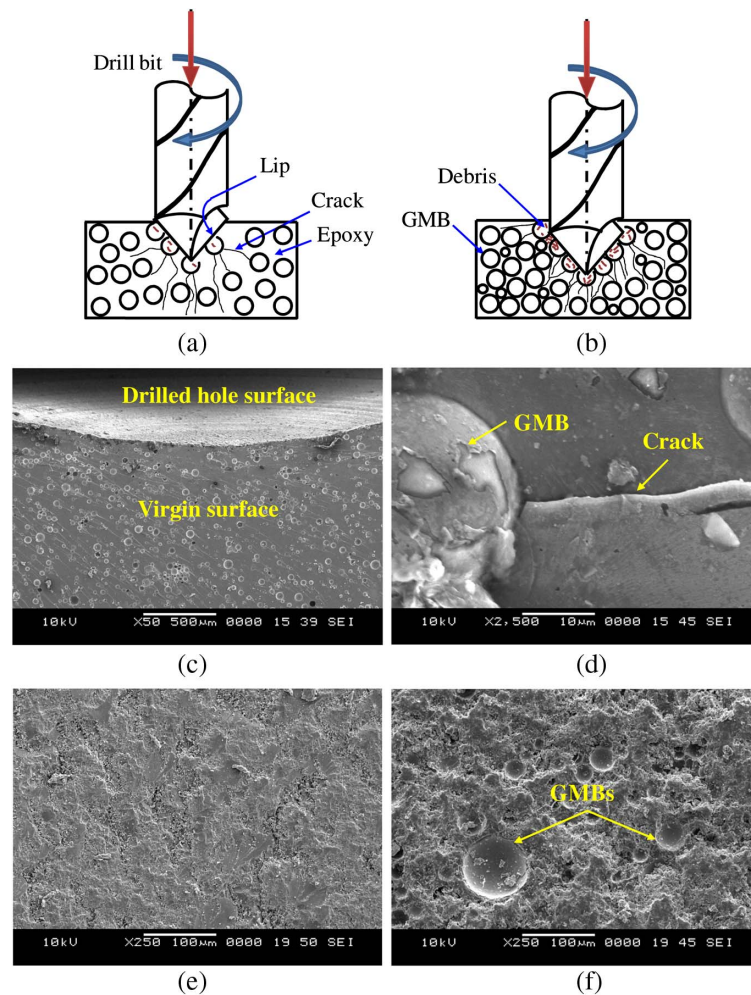

Fig. 2e). The specific cutting coefficient value increases with increase in the cutting speed and drill diameter but decreases with increase in the feed and filler content (see Table 4). The increase in the specific cutting coefficient is due to the increased thrust forces associated with a higher cutting speed and drill diameter. Increasing the filler content reduces the thrust forces, leading to reduced specific cutting coefficient values.

RSM-based models are proposed based on the experimental values (see Table 4) to predict intermediate values in the chosen range of input parameters and to capture the general trends. Furthermore, these models also help in analyzing interaction effects among various parameters.

MATHEMATICAL MODELS BASED ON EXPERIMENTAL DATA

The experimentally obtained values of epoxy specimens are superimposed on the plots for comparative analysis with the syntactic foam results. Regression equations are developed based on the experimental results using the commercially available Minitab Version 14 software (Minitab, Inc., State College, PA). The proposed models are obtained to predict

the thrust force (F_t), surface roughness (R_a), and specific cutting coefficient (K_f) as follows:

$$F_t = \begin{pmatrix} 26.3 - 0.225 \times v + 513 \times f - 0.084 \times R - 2.66 \times D + 0.000654 \\ \times v^2 - 3066 \times f^2 + 0.00954 \times R^2 + 0.511 \times D^2 + 1.907 \times v \times f - 0.00136 \times v \\ \times R + 0.00818 \times v \times D - 4.09 \times f \times R + 35.77 \times f \times D - 0.0988 \times R \times D \end{pmatrix} \quad (8)$$

$$R_a = \begin{pmatrix} 10.77 + 0.01748 \times v + 7.1 \times f + 0.0601 \times R - 1.831 \times D - 0.00004 \\ \times v^2 + 49.6 \times f^2 - 0.000392 \times R^2 + 0.07961 \times D^2 - 0.0026 \times v \times f + 0.000002 \\ \times v \times R - 0.000309 \times v \times D - 0.146 \times f \times R - 0.947 \times f \times D - 0.00188 \times R \times D \end{pmatrix} \quad (9)$$

$$K_f = \begin{pmatrix} 457.1 - 0.262 \times v - 3740 \times f - 4.24 \times R + 2.24 \times D + 0.00179 \\ \times v^2 + 13444 \times f^2 + 0.0199 \times R^2 + 0.505 \times D^2 + 3.22 \times v \times f - 0.00629 \times v \times R \\ + 0.0071 \times v \times D + 20.34 \times f \times R - 83.4 \times f \times D - 0.0585 \times R \times D \end{pmatrix} \quad (10)$$

Eqs 8–10 are used to predict intermediate values and trends within the chosen range of input parameters. The adequacy of these models is confirmed through ANOVA and is presented in Table 5. The F-ratio is the ratio of the mean square of the regression equation to the mean square of the residual error. For mathematical models to be adequate at a 99 % confidence level, the computed value of the F-ratio for Eqs 8–10 (164, 15, and 68, respectively) should be more than the corresponding value in the F-table (2.36). The coefficient of determination (CoD) is used to test the goodness of fit for the developed mathematical models, in which higher CoD values indicate a stronger correlation between the predicted and experimental values [23,43,44]. Fig. 3 presents the comparison between the experimental and predicted values, showing the close relationship between them. The average error is found to be 0.7 %, 3.6 %, and 0.7 % for F_t, R_a, and K_f, respectively. The developed models can be effectively used as a tool in industrial practices to predict the drilling characteristics of syntactic foams.

EFFECTS OF INDIVIDUAL PARAMETERS

The cutting speed, feed, drill diameter, and filler content are varied one at a time within the chosen range, keeping the other parameters at middle level in Eqs 8–10 to predict the trend and values of responses presented in Fig. 4. The thrust force increases with increases in the cutting speed, feed (see Fig. 4a), and drill diameter (see Fig. 4b) but decreases with increases in the filler loadings. The surface roughness increases with increases in the cutting speed but decreases with increases in the feed (see Fig. 4c) and filler content (see Fig. 4d). The surface roughness decreases with increases in the drill diameter up to 12 mm and later

TABLE 5
ANOVA results for machinability models for syntactic foams.

| Responses | Sum of Squares | | Degrees of Freedom | | Mean Square | | F-Ratio | CoD |
	Regression	Residual	Regression	Residual	Regression	Residual		
Thrust force	1.141×10^5	3,258.39	14	66	8,148.56	49.78	163.70[a]	0.9720
Surface roughness	48.83	15.65	14	66	3.49	0.24	14.71[a]	0.7574
Specific cutting coefficient	3.685×10^5	25,597.19	14	66	26,320.58	387.84	67.87[a]	0.9350

Note: [a] F-table = 2.36. Significance at 99 % confidence interval.

FIG. 3

Comparison between measured and predicted values for (a) F_t, (b) R_a, and (c) K_f.

(a)

(b)

(c)
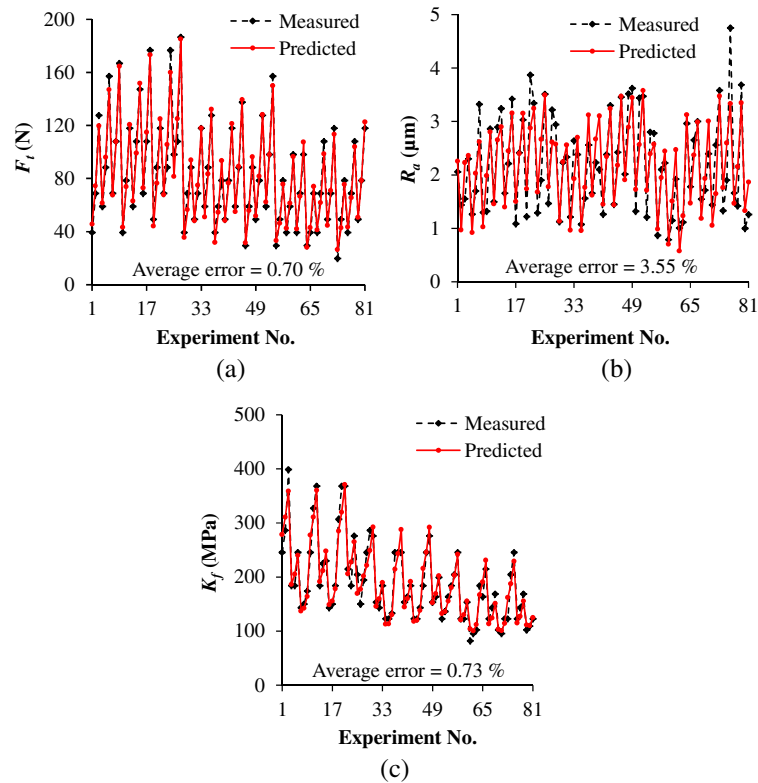
shows an increasing trend, as shown in **Fig. 4d**. **Fig. 4e** and **f** shows that K_f increases with the cutting speed and drill diameter but decreases with increases in the feed and filler content. These plots can serve as a reference to understand the general relationships among various parameters.

EFFECTS OF TWO-PARAMETER INTERACTIONS

Two parameters are varied at the same time in Eqs **8–10**, keeping the other two at their middle levels, as per the scheme presented in **Table 6** for the results presented in the following sections.

Thrust Force

Fig. 5a shows that the thrust force increases with the cutting speed and drill diameter. With the cutting speed increasing from v_{25}–v_{125}, F_t increases by 7.6 % and 8.7 % for D_8 and D_{16}, respectively. The variation of F_t with the increasing cutting speed is observed to be very small. A similar effect of cutting speed on F_t was observed in the drilling of epoxy matrix composites by Basavarajappa et al. [41]. The thrust force as a function of cutting speed and feed is presented in **Fig. 5b**. F_t increases by 1 % and 17 % for $f_{0.04}$ and $f_{0.12}$, respectively, with increases in the speed. The thrust force increases with the cutting speed but decreases with increases in R (see **Fig. 5c**). F_t decreases in the range of 52–58 %, as compared to neat epoxy, with increases in the cutting speed. As the drill advances in the syntactic foam specimen, axial and tangential forces exerted by the tool

FIG. 4

F_t as a function of (a) v and f and (b) R and D. R_a as a function of (c) v and f and (d) R and D. K_f as a function of (e) v and f and (f) R and D.
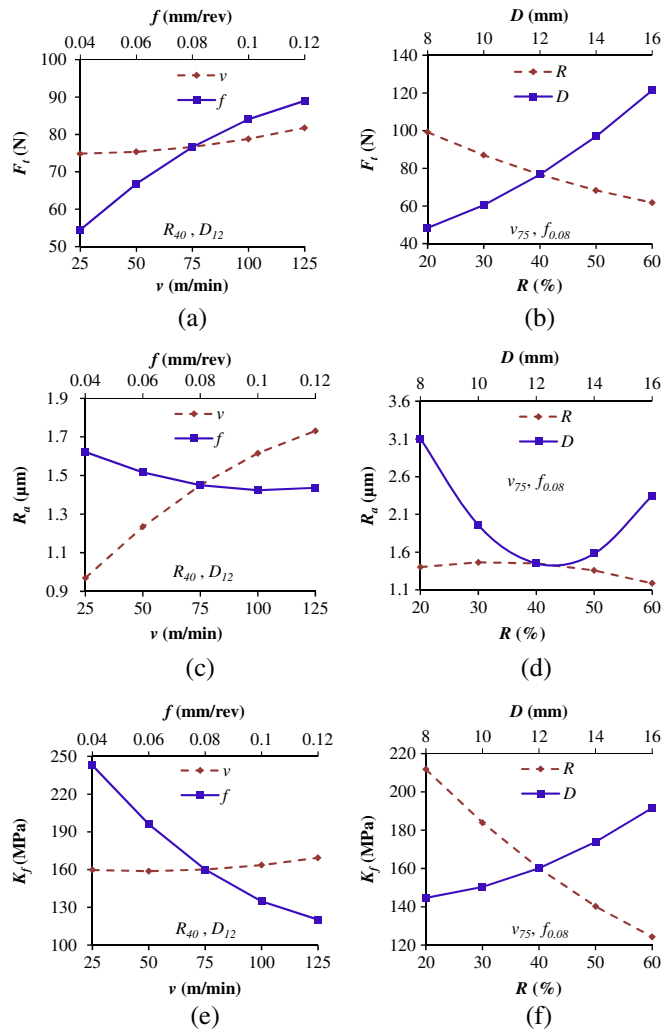

TABLE 6

Two-way interaction parameters used in the study for syntactic foams.

	Interaction	
Parameter 1	Parameter 2	Response
v	D, f, and R	F_t, R_a, and K_f
f	D and R	
R	D	

promote de-bonding between the particle and matrix. GMBs being relatively more brittle than the matrix, a large number of particles shear at higher filler loadings, resulting in a declining trend of F_t. The presence of a void inside GMBs leads to lower thrust forces, because the fracture of the particle exposes the void for the drill to advance without any resistance. The thrust force is found to increase with the feed and drill diameter

FIG. 5

Variation of F_t with respect to v for different (a) D, (b) f, and (c) R. F_t with respect to f at different (d) D and (e) R. (f) F_t with respect to D at different R.
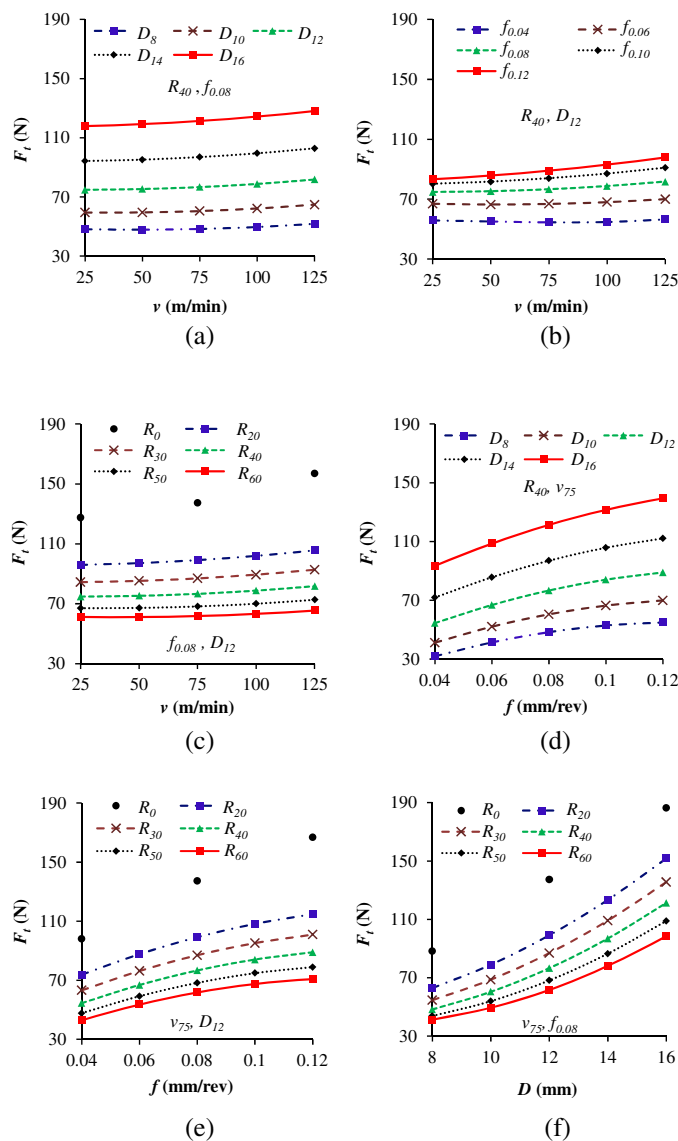
(see **Fig. 5d**). It increases in the range of 72–49 % with increases in the feed from $f_{0.04}$–$f_{0.12}$. At higher feeds, the resistance offered by the substrate rises in the direction of cutting, resulting in increased friction between the tool and substrate, leading to higher thrust forces. The material removal rate also increases due to an increased contact area, leading to higher values of F_t [38,41,45]. **Fig. 5e** shows the variation of feed and filler content as a function of thrust force. The thrust force increases with increasing feed and decreasing filler content. The thrust force reduces by 56–58 % compared to that of neat epoxy with an increasing feed from $f_{0.04}$–$f_{0.12}$. The variation of F_t with the drill diameter and filler content is presented in **Fig. 5f**. With the drill diameter increasing from D_8–D_{16}, F_t

increases in the range of 141–139 %. As the drill diameter increases, the contact area of the drilled hole increases, leading to higher F_t [19, 36].

Surface Roughness

The surface roughness increases with the increasing cutting speed at all levels of drill diameter (see **Fig. 6a**). It increases by 35 % and 33 % for D_8 and D_{16}, respectively, with higher cutting speeds. The temperature rises at the tool–specimen interface with increases in the cutting speed, leading to increased surface roughness [23,42,46]. The surface roughness increases with the cutting speed but decreases with the increasing feed (see **Fig. 6b**). R_a increases by 69 % and 79 % for $f_{0.04}$ and $f_{0.12}$, respectively, with increases in the cutting speed. **Fig. 6c** exhibits the effect of filler content on R_a. In comparison to R_a of neat epoxy, roughness in foams is observed to be increased by 5.8 and 8.8 times with increases in the cutting speed. Nevertheless, in foams, the surface roughness decreases (24–13 %) with increases in the filler content, owing to the burnishing and honing effect produced by abrasive fillers [41]. Additionally, the lower thrust force with increased R results in reduced

FIG. 6

Variation of R_a with respect to v for different (a) D, (b) f, and (c) R. R_a with respect to f at different (d) D and (e) R. (f) R_a with respect to D at different R.
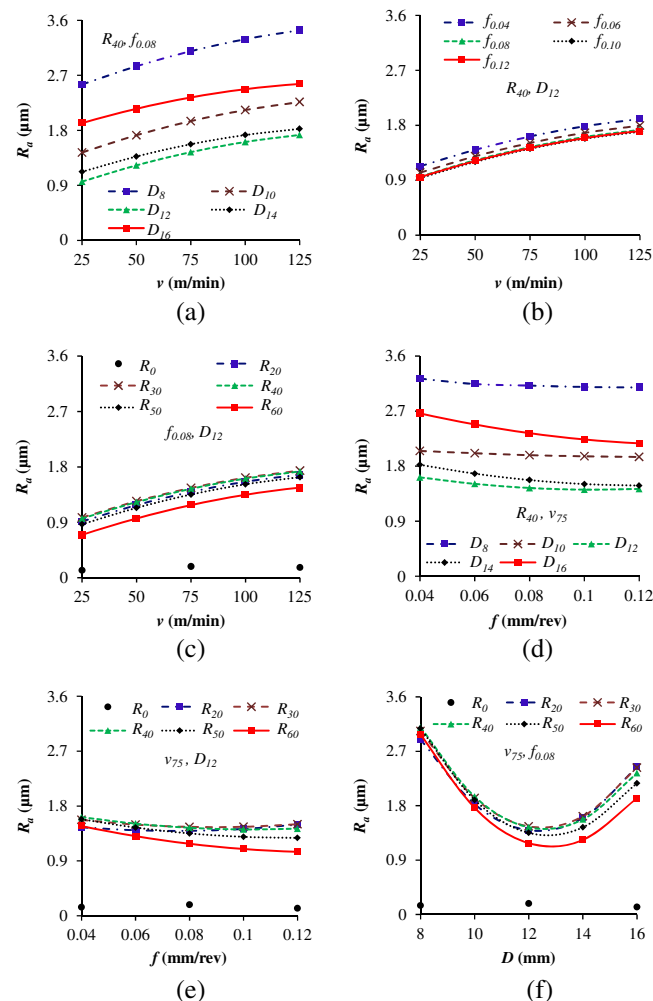
surface roughness [22,23,39,47]. **Fig. 6d** shows a decrease in R_a by 4.5 % and 18.5 % for D_8 and D_{16}, respectively, with increases in the feed. At a higher feed, the temperature decreases because of reduced contact time between the tool and samples, leading to lower R_a [42,46]. The surface roughness decreases with increases in the feed and filler content, as observed from **Fig. 6e**. R_a increases by over 9 times as compared to neat epoxy, with the feed increasing from $f_{0.04}$–$f_{0.12}$. R_a decreases by 52–60 % with increases in the drill diameter up to D_{12} for $f_{0.04}$–$f_{0.12}$ and is later found to be increased (see **Fig. 6f**). At any given cutting speed, D_{12} has a lower spindle speed than D_8 ($N = 1{,}000\ v/\pi D$), which results in lower R_a [23,48]. Beyond D_{12}, the surface roughness increases because of higher F_t values [19,36].

Specific Cutting Coefficient

K_f increases with the cutting speed and drill diameter, as observed in **Fig. 7a**. With the increasing cutting speed, K_f increases by 5 % and 7 % for D_8 and D_{16}, respectively.

FIG. 7

Variation of K_f with respect to v for different (a) D, (b) f, and (c) R. K_f with respect to f at different (d) D and (e) R. (f) K_f with respect to D at different R.
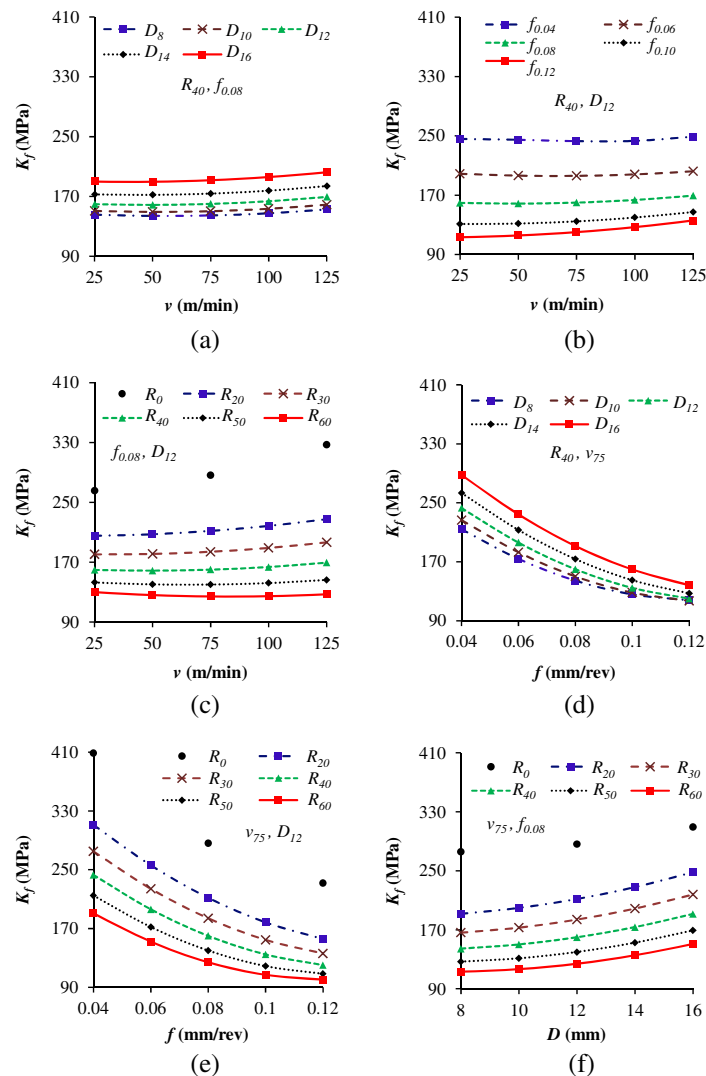
TABLE 7

Input parameter settings for specific responses in the drilling performance of syntactic foams.

	Minimum	Maximum
F_t	$v_{125}f_{0.04}D_8R_{60}$	$v_{125}f_{0.12}D_{16}R_{20}$
R_a	$v_{25}f_{0.08}D_{12}R_{60}$	$v_{125}f_{0.08}D_8R_{20}$
K_f	$v_{25}f_{0.12}D_8R_{60}$	$v_{25}f_{0.04}D_{16}R_{20}$

Increased thrust force at a higher cutting speed is the likely reason for increased K_f [49]. K_f increases by 1 % and 20 % for $f_{0.04}$ and $f_{0.12}$ with increasing speed (see **Fig. 7b**). **Fig. 7c** shows that K_f increases with increases in v and decreases in R. K_f is observed to decrease in the range of 51–61 %, as compared to neat epoxy, with increases in speed. Lower K_f is due to reduced F_t with increases in R [41,49,50]. **Fig. 7d** shows the variation of K_f with f and D. The specific cutting coefficient decreases with increases in the feed and decreases in the drill diameter. At low feeds, the material is subjected to lower strain rates, leading to an

FIG. 8 Micrographs of (a) neat epoxy and (b) E60 at the same magnification. Types of chips formed at different cutting speeds and feeds in the drilling of (c) neat epoxy and (d) E60 for D_{16}.
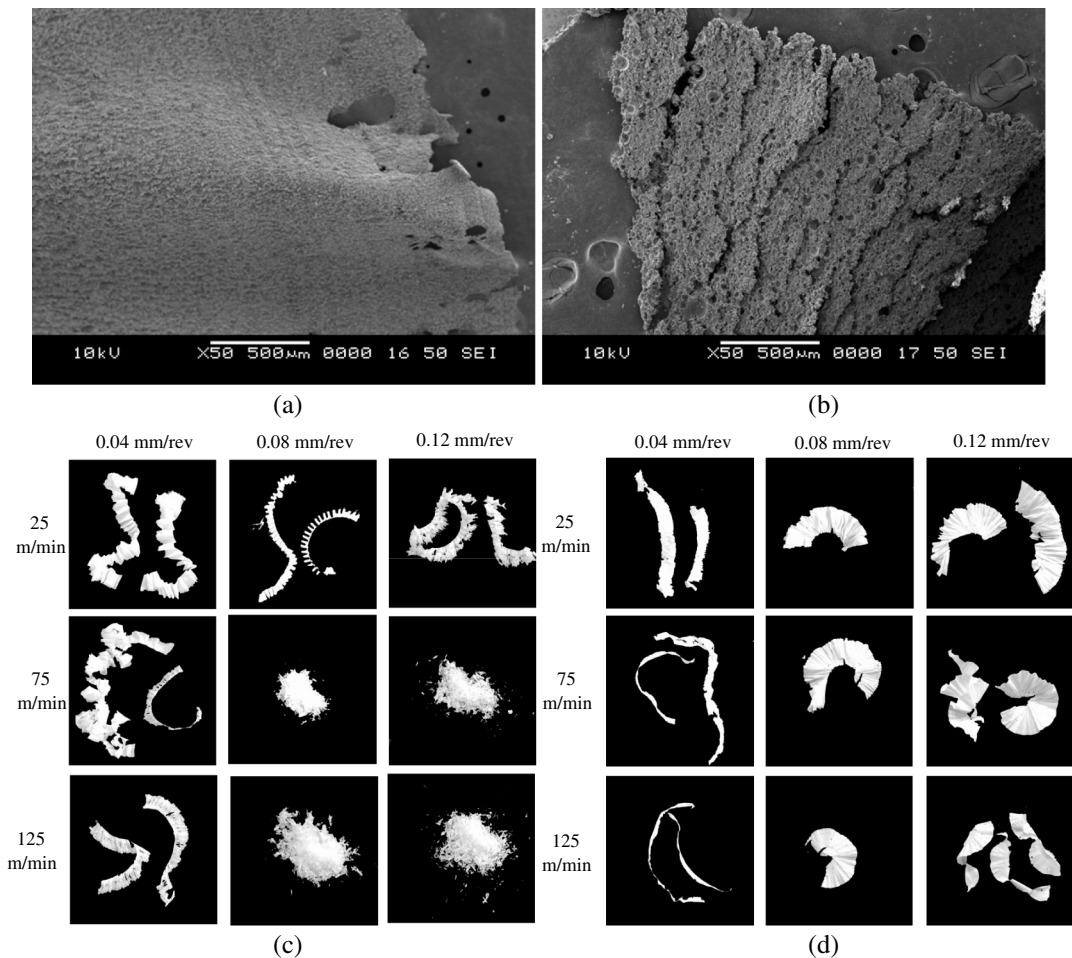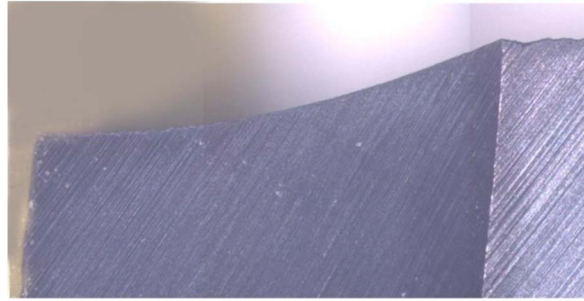
FIG. 9

Confocal microscope image
post-drilling operation.

increased specific cutting coefficient [38,41]. **Fig. 7e** shows the variation of the specific cutting coefficient with R at various feeds. K_f in foam decreases in the range of 53–57 %, as compared to neat epoxy, with increases in the feed from $f_{0.04}$–$f_{0.12}$. The specific cutting coefficient increases with increases in the drill diameter and decreases in the filler content (see **Fig. 7f**). Increases in the drill diameter increase K_f by 29 % and 33 % for R_{20} and R_{60}, respectively. Increases in the thrust force with an increasing drill diameter results in higher K_f [49,51].

Input parameter settings based on the experimental investigations (see **Table 4**), for a specific response in the drilling performance of syntactic foams, are summarized in **Table 7**. Filler content strongly influences the machinability characteristics of syntactic foams, as observed in this table. Higher GMB content is preferred in the foams from a drilling operations perspective, which is also beneficial for weight-sensitive applications.

CHIP MORPHOLOGY AND TOOL WEAR

Low-magnification micrographs of chips formed from neat epoxy and E60 are presented in **Fig. 8a** and **b**, respectively. The foam chips have fractured in multiple places, unlike the neat epoxy chips. Foam chips are desired, as they are easily removed from the machined surfaces, avoiding entanglement around the cutting tool. **Fig. 8c** shows representative images of neat epoxy chips produced in drilling at different cutting speeds and feeds for D_{16}. Ribbons are formed at a lower feed, and increasing the speed did not show any significant effect on the chip morphology. Washer-type helical chips [52] are formed until $f_{0.08}$, but a higher feed results in discontinuous ribbon-type chips. At intermediate levels of feed and speed, powdery chips are formed. This ductile-to-brittle transition in the chip forming mechanism in neat epoxy specimens is interesting. Chips formed in the drilling of syntactic foam at different cutting speeds and feeds are presented in **Fig. 8d**. Ribbon-type chips are formed in all the syntactic foams, unlike powdery ones under some conditions in neat epoxy. **Fig. 9** presents a confocal microscopic image of the cutting tool used in this work post-drilling operation. No signs of tool wear are seen from this image, though GMB is brittle and abrasive in nature.

Conclusions

GMB/epoxy syntactic foams are studied for machinability characteristics under drilling conditions. The study parameters include the thrust force, surface roughness, and specific

cutting coefficient. The cutting speed, feed, drill diameter, and filler content are varied in the study. The following conclusions are drawn within the ranges of the selected parameters:

- F_t increases with an increase in v, f, and D but decreases with filler content. The thrust force generated in the drilling of syntactic foams is 39.8 % lower than that of neat epoxy.
- R_a increases with an increasing cutting speed but decreases with feed and filler content. Surface roughness decreases up to a certain drill diameter and then increases.
- The specific cutting coefficient increases with an increasing cutting speed and drill diameter, whereas it decreases with feed and filler content. In comparison to neat epoxy, the specific cutting coefficient of syntactic foams decreases by 40 %.
- Optimum input parameter settings based on RSM for minimizing the responses are as follows:
  - F_t: $v_{125}f_{0.04}D_8R_{60}$
  - R_a: $v_{25}f_{0.08}D_{12}R_{60}$
  - K_f: $v_{25}f_{0.12}D_8R_{60}$
- The surface roughness of holes in syntactic foams decreases with increasing GMB content because of the burnishing and honing effect produced by abrasive particles.
- Among the chosen input parameters, drill diameter is found to be most influential on F_t and R_a, whereas K_f is governed by feed, followed by filler content.

References

[1] Bardella, L., Sfreddo, A., Ventura, C., Porfiri, M., and Gupta, N., "A Critical Evaluation of Micromechanical Models for Syntactic Foams," *Mech. Mater.*, Vol. 50, 2012, pp. 53–69, https://doi.org/10.1016/j.mechmat.2012.02.008

[2] Gupta, N., Kishore, Woldesenbet, E., and Sankaran, S., "Studies on Compressive Failure Features in Syntactic Foam Material," *J. Mater. Sci.*, Vol. 36, No. 18, 2001, pp. 4485–4491, https://doi.org/10.1023/A:1017986820603

[3] Panteghini, A. and Bardella, L., "On the Compressive Strength of Glass Microballoons-Based Syntactic Foams," *Mech. Mater.*, Vol. 82, 2015, pp. 63–77, https://doi.org/10.1016/j.mechmat.2014.12.005

[4] Bharath Kumar, B. R., Doddamani, M., Zeltmann, S. E., Gupta, N., Uzma, Gurupadu, S., and Sailaja, R. R. N., "Effect of Particle Surface Treatment and Blending Method on Flexural Properties of Injection-Molded Cenosphere/HDPE Syntactic Foams," *J. Mater. Sci.*, Vol. 51, No. 8, 2016, pp. 3793–3805, https://doi.org/10.1007/s10853-015-9697-2

[5] Bharath Kumar, B. R., Singh, A. K., Doddamani, M., Luong, D. D., and Gupta, N., "Quasi-Static and High Strain Rate Compressive Response of Injection-Molded Cenosphere/HDPE Syntactic Foam," *JOM*, Vol. 68, No. 7, 2016, pp. 1861–1871, https://doi.org/10.1007/s11837-016-1912-3

[6]   Bharath Kumar, B. R., Doddamani, M., Zeltmann, S. E., Gupta, N., and Ramakrishna, S., "Data Characterizing Tensile Behavior of Cenosphere/HDPE Syntactic Foam," *Data Brief*, Vol. 6, 2016, pp. 933–941, https://doi.org/10.1016/j.dib.2016.01.058

[7]   Doddamani, M., Kishore, Shunmugasamy, V. C., Gupta, N., and Vijayakumar, H. B., "Compressive and Flexural Properties of Functionally Graded Fly Ash Cenosphere-Epoxy Resin Syntactic Foams," *Polym. Compos.*, Vol. 36, No. 4, 2015, pp. 685–693, https://doi.org/10.1002/pc.22987

[8]   Bharath Kumar, B. R., Zeltmann, S. E., Doddamani, M., Gupta, N., Uzma, Gurupadu, S., and Sailaja, R. R. N., "Effect of Cenosphere Surface Treatment and Blending Method on the Tensile Properties of Thermoplastic Matrix Syntactic Foams," *J. Appl. Polym. Sci.*, Vol. 133, No. 35, 2016, 43881, https://doi.org/10.1002/app.43881

[9]   Shahapurkar, K., Garcia, C. D., Doddamani, M., Mohan Kumar, G. C., and Prabhakar, P., "Compressive Behavior of Cenosphere/Epoxy Syntactic Foams in Arctic Conditions," *Composites Part B*, Vol. 135, 2018, pp. 253–262, https://doi.org/10.1016/j.compositesb.2017.10.006

[10] Gupta, N., Pinisetty, D., and Shunmugasamy, V. C., *Reinforced Polymer Matrix Syntactic Foams: Effect of Nano and Micro-Scale Reinforcement*, Springer International Publishing, New York, NY, 2013, 80p.

[11] Gupta, N., Zeltmann, S. E., Shunmugasamy, V. C., and Pinisetty, D., "Applications of Polymer Matrix Syntactic Foams," *JOM*, Vol. 66, No. 2, 2014, pp. 245–254, https://doi.org/10.1007/s11837-013-0796-8

[12] Li, P., Petrinic, N., Siviour, C., Froud, R., and Reed, J. M., "Strain Rate Dependent Compressive Properties of Glass Microballoon Epoxy Syntactic Foams," *Mater. Sci. Eng., A*, Vol. 515, Nos. 1–2, 2009, pp. 19–25, https://doi.org/10.1016/j.msea.2009.02.015

[13] Jayavardhan, M. L. and Doddamani, M., "Quasi-Static Compressive Response of Compression Molded Glass Microballoon/HDPE Syntactic Foam," *Composites Part B*, Vol. 149, 2018, pp. 165–177, https://doi.org/10.1016/j.compositesb.2018.04.039

[14] Manakari, V., Parande, G., and Gupta, M., "Effects of Hollow Fly-Ash Particles on the Properties of Magnesium Matrix Syntactic Foams: A Review," *Mater. Perform. Charact.*, Vol. 5, No. 1, 2016, pp. 116–131, https://doi.org/10.1520/MPC20150060

[15] Zeltmann, S. E., Chen, B., and Gupta, N., "Mechanical Properties of Epoxy Matrix-Borosilicate Glass Hollow-Particle Syntactic Foams," *Mater. Perform. Charact.*, Vol. 6, No. 1, 2017, pp. 1–16, https://doi.org/10.1520/MPC20150056

[16] Capello, E., Langella, A., Nele, L., Paoletti, A., Santo, L., and Tagliaferri, V., "Drilling Polymeric Matrix Composites," *Machining: Fundamentals and Recent Advances*, Springer, London, UK, 2008, pp. 167–194.

[17] Khashaba, U. A., "Drilling of Polymer Matrix Composites: A Review, " *J. Compos. Mater.*, Vol. 47, No. 15, 2013, pp. 1817–1832, https://doi.org/10.1177/0021998312451609

[18] Lin, S. C. and Chen, I. K., "Drilling Carbon Fiber-Reinforced Composite Material at High Speed," *Wear*, Vol. 194, Nos. 1–2, 1996, pp. 156–162, https://doi.org/10.1016/0043-1648(95)06831-7

[19] El-Sonbaty, I., Khashaba, U. A., and Machaly, T., "Factors Affecting the Machinability of GFR/Epoxy Composites," *Compos. Struct.*, Vol. 63, Nos. 3–4, 2004, pp. 329–338.

[20] Mohan, N. S., Ramachandra, A., and Kulkarni, S. M., "Influence of Process Parameters on Cutting Force and Torque during Drilling of Glass–Fiber Polyester Reinforced Composites," *Compos. Struct.*, Vol. 71, Nos. 3–4, 2005, pp. 407–413, https://doi.org/10.1016/j.compstruct.2005.09.039

[21] Kilickap, E., "Optimization of Cutting Parameters on Delamination Based on Taguchi Method during Drilling of GFRP Composite," *Expert Syst. Appl.*, Vol. 37, No. 8, 2010, pp. 6116–6122, https://doi.org/10.1016/j.eswa.2010.02.023

[22] Palanikumar, K., "Experimental Investigation and Optimisation in Drilling of GFRP Composites," *Measurement*, Vol. 44, No. 10, 2011, pp. 2138–2148, https://doi.org/10.1016/j.measurement.2011.07.023

[23] Gaitonde, V., Karnik, S. R., Rubio, J. C., Abrão, A. M., Correia, A. E., and Davim, J. P., "Surface Roughness Analysis in High-Speed Drilling of Unreinforced and Reinforced

Polyamides," *J. Compos. Mater.*, Vol. 46, No. 21, 2012, pp. 2659–2673, https://doi.org/10.1177/0021998311431640

[24] Krishnaraj, V., Prabukarthi, A., Ramanathan, A., Elanghovan, N., Kumar, M. S., Zitoune, R., and Davim, J. P., "Optimization of Machining Parameters at High Speed Drilling of Carbon Fiber Reinforced Plastic (CFRP) Laminates," *Composites Part B*, Vol. 43, No. 4, 2012, pp. 1791–1799, https://doi.org/10.1016/j.compositesb.2012.01.007

[25] Rubio, J. C. C., da Silva, L. J., de Oliveira Leite, W., Panzera, T. H., Ribeiro Filho, S. L. M., and Davim, J. P., "Investigations on the Drilling Process of Unreinforced and Reinforced Polyamides Using Taguchi Method," *Composites Part B*, Vol. 55, 2013, pp. 338–344, https://doi.org/10.1016/j.compositesb.2013.06.042

[26] Kuram, E., "Micro-Machinability of Injection Molded Polyamide 6 Polymer and Glass-Fiber Reinforced Polyamide 6 Composite," *Composites Part B*, Vol. 88, 2016, pp. 85–100, https://doi.org/10.1016/j.compositesb.2015.11.004

[27] Faria, P. E., Campos, R. F., Abrão, A. M., Godoy, G. C. D., and Davim, J. P., "Thrust Force and Wear Assessment when Drilling Glass Fiber-Reinforced Polymeric Composite," *J. Compos. Mater.*, Vol. 42, No. 14, 2008, pp. 1401–1414, https://doi.org/10.1177/0021998308090456

[28] Ismail, S. O., Ojo, S. O., and Dhakal, H. N., "Thermo-Mechanical Modelling of FRP Cross-Ply Composite Laminates Drilling: Delamination Damage Analysis," *Composites Part B*, Vol. 108, 2017, pp. 45–52, https://doi.org/10.1016/j.compositesb.2016.09.100

[29] Ojo, S. O., Ismail, S. O., Paggi, M., and Dhakal, H. N., "A New Analytical Critical Thrust Force Model for Delamination Analysis of Laminated Composites during Drilling Operation," *Composites Part B*, Vol. 124, 2017, pp. 207–217, https://doi.org/10.1016/j.compositesb.2017.05.039

[30] Shunmugasamy, V. C., Zeltmann, S. E., Gupta, N., and Strbik, O. M., III, "Compressive Characterization of Single Porous SiC Hollow Particles," *JOM*, Vol. 66, No. 6, 2014, pp. 892–897, https://doi.org/10.1007/s11837-014-0954-7

[31] Tagliavia, G., Porfiri, M., and Gupta, N., "Analysis of Flexural Properties of Hollow-Particle Filled Composites," *Composites Part B*, Vol. 41, No. 1, 2010, pp. 86–93, https://doi.org/10.1016/j.compositesb.2009.03.004

[32] Jayavardhan, M. L., Bharath Kumar, B. R., Doddamani, M., Singh, A. K., Zeltmann, S. E., and Gupta, N., "Development of Glass Microballoon/HDPE Syntactic Foams by Compression Molding," *Composites Part B*, Vol. 130, 2017, pp. 119–131, https://doi.org/10.1016/j.compositesb.2017.07.037

[33] Gupta, N. and Nagorny, R., "Tensile Properties of Glass Microballoon-Epoxy Resin Syntactic Foams," *J. Appl. Polym. Sci.*, Vol. 102, No. 2, 2006, pp. 1254–1261, https://doi.org/10.1002/app.23548

[34] Montgomery, D., *Design and Analysis of Experiments*, Wiley, Hoboken, NJ, 2003, 696p.

[35] Gaitonde, V. N., Karnik, S. R., Rubio, J. C., Correia, A. E., Abrão, A. M., and Davim, J. P., "Analysis of Parametric Influence on Delamination in High-Speed Drilling of Carbon Fiber Reinforced Plastic Composites," *J. Mater. Process. Technol.*, Vol. 203, Nos. 1–3, 2008, pp. 431–438, https://doi.org/10.1016/j.jmatprotec.2007.10.050

[36] Rajamurugan, T. V., Shanmugam, K., and Palanikumar, K., "Analysis of Delamination in Drilling Glass Fiber Reinforced Polyester Composites," *Mater. Des.*, Vol. 45, 2013, pp. 80–87, https://doi.org/10.1016/j.matdes.2012.08.047

[37] Davim, J. P., Gaitonde, V. N., and Karnik, S. R., "An Investigative Study of Delamination in Drilling of Medium Density Fibreboard (MDF) Using Response Surface Models," *Int. J. Adv. Manuf. Technol.*, Vol. 37, Nos. 1–2, 2008, pp. 49–57, https://doi.org/10.1007/s00170-007-0937-8

[38] Gaitonde, V. N., Karnik, S. R., Mata, F., and Davim, J. P., "Study on Some Aspects of Machinability in Unreinforced and Reinforced Polyamides," *J. Compos. Mater.*, Vol. 43, No. 7, 2009, pp. 725–739, https://doi.org/10.1177/0021998309101298

[39] Palanikumar, K. and Karthikeyan, R., "Assessment of Factors Influencing Surface Roughness on the Machining of Al/SiC Particulate Composites," *Mater. Des.*, Vol. 28, No. 5, 2007, pp. 1584–1591, https://doi.org/10.1016/j.matdes.2006.02.010

[40] Karnik, S. R. and Gaitonde, V. N., "Development of Artificial Neural Network Models to Study the Effect of Process Parameters on Burr Size in Drilling," *Int. J. Adv. Manuf. Technol.*, Vol. 39, Nos. 5–6, 2008, pp. 439–453, https://doi.org/10.1007/s00170-007-1231-5

[41] Basavarajappa, S., Venkatesh, A., Gaitonde, V. N., and Karnik, S. R., "Experimental Investigations on Some Aspects of Machinability in Drilling of Glass Epoxy Polymer Composites," *J. Thermoplast. Compos. Mater.*, Vol. 25, No. 3, 2012, pp. 363–387, https://doi.org/10.1177/0892705711408166

[42] Giasin, K., Ayvar-Soberanis, S., and Hodzic, A., "An Experimental Study on Drilling of Unidirectional GLARE Fibre Metal Laminates," *Compos. Struct.*, Vol. 133, 2015, pp. 794–808, https://doi.org/10.1016/j.compstruct.2015.08.007

[43] Manakari, V., Parande, G., Doddamani, M., Gaitonde, V. N., Siddhalingeshwar, I. G., Kishore, Shunmugasamy, V. C., and Gupta, N., "Dry Sliding Wear of Epoxy/Cenosphere Syntactic Foams," *Tribol. Int.*, Vol. 92, 2015, pp. 425–438, https://doi.org/10.1016/j.triboint.2015.07.026

[44] Gaitonde, V. N., Karnik, S. R., Rubio, J. C. C., de Oliveira Leite, W., and Davim, J. P., "Experimental Studies on Hole Quality and Machinability Characteristics in Drilling of Unreinforced and Reinforced Polyamides," *J. Compos. Mater.*, Vol. 48, No. 1, 2014, pp. 21–36, https://doi.org/10.1177/0021998312467552

[45] Ravichandran, G., Raju, K., Varadarajan, Y., and Suresha, B., "Performance of HSS and Carbide Drills on Micro Filler Filled Glass Fabric Reinforced Epoxy Composites," *Polym. Res. J.*, Vol. 10, No. 4, 2016, pp. 175–185.

[46] Rubio, J. C. C., Abrão, A. M., Faria, P. E., Correia, A. E., and Davim, J. P., "Delamination in High Speed Drilling of Carbon Fiber Reinforced Plastic (CFRP)," *J. Compos. Mater.*, Vol. 42, No. 15, 2008, pp. 1523–1532, https://doi.org/10.1177/0021998308092205

[47] Rubio, J. C., Panzera, T. H., Abrao, A., Faria, P. E., and Davim, J. P., "Effects of High Speed in the Drilling of Glass Whisker-Reinforced Polyamide Composites (PA66 GF30): Statistical Analysis of the Roughness Parameters," *J. Compos. Mater.*, Vol. 45, No. 13, 2011, pp. 1395–1402, https://doi.org/10.1177/0021998310381540

[48] Khashaba, U. A., El-Sonbaty, I. A., Selmy, A. I., and Megahed, A. A., "Machinability Analysis in Drilling Woven GFR/Epoxy Composites: Part I—Effect of Machining Parameters," *Composites Part A*, Vol. 41, No. 3, 2010, pp. 391–400, https://doi.org/10.1016/j.compositesa.2009.11.006

[49] Davim, J. P., Reis, P., Lapa, V., and António, C. C., "Machinability Study on Polyetheretherketone (PEEK) Unreinforced and Reinforced (GF30) for Applications in Structural Components," *Compos. Struct.*, Vol. 62, No. 1, 2003, pp. 67–73, https://doi.org/10.1016/S0263-8223(03)00085-0

[50] Davim, J. P., Silva, L. R., Festas, A., and Abrão, A. M., "Machinability Study on Precision Turning of PA66 Polyamide with and without Glass Fiber Reinforcing," *Mater. Des.*, Vol. 30, No. 2, 2009, pp. 228–234, https://doi.org/10.1016/j.matdes.2008.05.003

[51] Gaitonde, V. N., Karnik, S. R., Mata, F., and Davim, J. P., "Modeling and Analysis of Machinability Characteristics in PA6 and PA66 GF30 Polyamides through Artificial Neural Network," *J. Thermoplast. Compos. Mater.*, Vol. 23, No. 3, 2010, pp. 313–336, https://doi.org/10.1177/0892705709349319

[52] Knight, W. A. and Boothroyd, G., *Fundamentals of Metal Machining and Machine Tools*, 3rd ed., CRC Press, Boca Raton, FL, 2005, 602p.